J. Physiol. (1959) 145, 505–528

THE ELECTRICAL CONSTANTS OF THE MOTONEURONE MEMBRANE

By J. S. COOMBS, D. R. CURTIS and J. C. ECCLES

From the Department of Physiology, Australian National University, Canberra

(*Received* 3 *September* 1958)

Araki & Otani (1955) have recorded the time course of the potential change developed across the membrane of toad motoneurones when a rectangular current pulse was applied through an intracellular micro-electrode. A bridge circuit was used to balance out the complicating potential changes produced in the micro-electrode and other structures in series with the motoneurone membrane. In this way it was possible to derive values for the resistance and electric time constant of this membrane. Frank & Fuortes (1956) found that on account of electrode polarization this method was unreliable with the micro-electrodes which they inserted into cat motoneurones. Consequently they adopted more indirect methods, which will be discussed later in this paper in relation to values for these motoneurones that have been obtained by methods similar to those of Araki & Otani and also by the double-barrel micro-electrodes developed by Coombs, Eccles & Fatt (1955). Furthermore, in interpreting the results an attempt has been made to allow for the distortion introduced by the complex morphology of the motoneurone (cf. Rall, 1957). Finally, the measurements of the electrical constants of cat motoneurones will be considered in relationship to measurements made with three investigations on other types of nerve cells. Ito (1957) investigated toad spinal ganglion cells by a method developed from that of Araki & Otani (1955). Tauc (1955, 1956, 1957) and Fessard & Tauc (1956) succeeded in inserting two independent micro-electrodes into the giant ganglion cells of *Aplysia depilans* or *punctata* and *Helix pomatia*, and thus were able to apply currents through one electrode and with the other to measure potentials that were virtually uncomplicated by coupling between the electrodes. Similar investigations have recently been reported on cardiac ganglion cells of lobster (*Panulirus interruptus*) by Otani & Bullock (1957) and on the supramedullary neurones of the puffer fish

(*Spheroides vermicularis*) by Hagiwara & Saito (1957). A preliminary account of part of the present investigation has been published (Coombs, Curtis & Eccles, 1956).

METHODS

All experiments were performed on motoneurones of the lower lumbar segments of the cat's spinal cord. Light pentobarbital anaesthesia was used and the cord was transected in the lower thoracic region. The techniques of dissection and micromanipulation have been described in earlier publications (Eccles, Fatt, Landgren & Winsbury, 1954).

Micro-electrodes

Both single- and double-barrelled electrodes were used (Coombs *et al.* 1955) and were filled with either 3 M-KCl or 0·6 M-K_2SO_4 solutions. After filling, the resistances of the electrodes were determined with their tips immersed in NaCl solution 0·9 % (w/v) and only those with resistances of 5–15 MΩ were used in the experiments. The difficulties associated with the use of double-barrelled micro-electrodes have been described (Coombs *et al.* 1955). In particular, the passage of the electrode through the tissues of the spinal cord produces fluctuations in the resistive coupling between the barrels and hence uncontrollable artifacts when current through one barrel is used to alter the membrane potential of an impaled cell. Electrodes having values of 50–200 kΩ for this coupling resistance were selected. The coupling resistance tended to be lower when double electrodes were fashioned by fusing two glass tubes side by side before pulling than when they were made by the method of inserting a septum into a tube (Coombs *et al.* 1955). Micro-electrodes often suffered large permanent increases in resistance during the passage through spinal tissue, an effect which was particularly frequent with electrodes filled with K_2SO_4 solution. To some extent this difficulty was overcome by filling the electrodes with concentrated electrolyte solutions containing 1 % agar (Difco). It is possible that this semi-solid medium prevented the mechanical blocking of the orifice of the electrode by poorly conducting material, particularly myelin.

Recording equipment

Connexion of the micro-electrode with the electrical equipment was made through an Ag–AgCl junction. The indifferent lead from the cat (earth plate) was made also through an Ag–AgCl junction and a saline-soaked cotton gauze pad which made a low-resistance contact with the lumbar muscles.

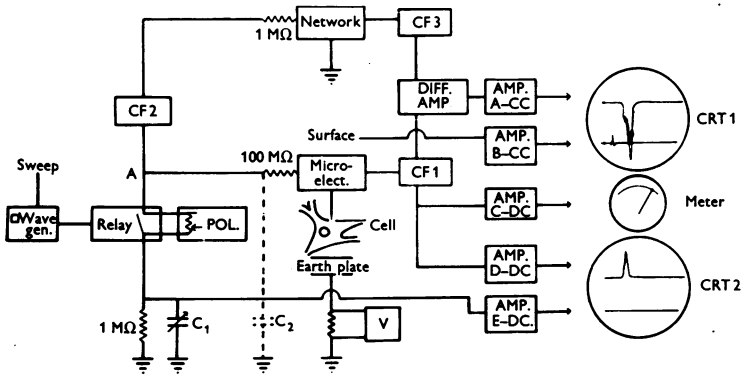

Fig. 1. Block diagram of the electrical and display equipment. Amplifiers A to E are either direct-coupled (DC) or capacitively-coupled (CC). For further details see text.

Fig. 1 is a block diagram of the electrical and display equipment used. The micro-electrode was attached to a small probe unit containing a cathode follower input stage (CF 1) which was itself rightly fixed to the micromanipulator. This input stage was connected to three amplifiers. Two

direct-coupled units of fixed low gain (AMP. C, AMP. D) recorded the membrane resting potential, AMP. C giving a meter reading and AMP. D feeding the upper beam of one cathode ray tube (CRT 2). This latter beam would, of course, also record transient changes in membrane potential, e.g. action potentials. The third amplifier had a differential input and controlled the upper beam of another cathode ray tube (CRT 1) by means of a capacitively-coupled unit (AMP. A) having a greater range of amplification. The time constant of this unit was adjustable, but a value of at least 200 msec was always used when recording spikes and post-synaptic potentials which would thereby suffer only a negligible distortion. Potential changes, led from the dorsal surface of the spinal cord by platinum electrodes, were also amplified by another capacitively-coupled amplifier (AMP. B) and recorded on the lower beam of CRT 1. Two synchronized Grass Kymograph cameras were used to photograph the CRT's, and AMP. C was usually also connected to an Esterline-Angus recording voltmeter.

Electrical properties of the motoneurone membrane

Since the surface membranes of giant axons and of muscle fibres have been shown to approximate to a simple electrical system composed of resistance and capacity elements in parallel (Katz, 1948; Hodgkin, 1951), it is likely that the surface membranes of the soma, dendrites and initial segment of the motoneurone would exhibit comparable properties. Consequently, the most direct method of measuring the values of the capacity and resistance of such a system would be to record with a micro-electrode the time course and size of the potential generated by the passage of a rectangular current pulse across the membrane (cf. Araki & Otani 1955; Ito, 1957). Because of inherent technical difficulties a fraction of this current must also pass through the recording electrode, be it single- or double-barrelled. Since the neuronal membrane has a resistance of less than 10% of the electrode resistance, the total observed potential change with a single electrode will be dominated by the electrical properties of the electrode. Further, in order to determine the time constant of the membrane, it is essential to be able to record the potential changes that occur across the membrane as soon as possible after the onset of the current pulse. Both with single and double electrodes considerable voltages have to be applied in order to obtain the necessary currents. In the case of the single electrode this voltage is applied directly to the input grid of CF 1, while with the double electrode a large artifact will appear in the recording barrel, due to the capacitive coupling between barrels (cf. Coombs *et al.* 1955).

Consequently, if it be assumed that the electrode properties are not altered during the passage of current, both the steady potential due to current flow through the electrode itself and the potential due to application of a current pulse either directly or indirectly to the grid of CF 1 could be balanced out by a bridge circuit (cf. Araki & Otani, 1955; Ito, 1957). A network was designed to reproduce potentials that could exactly balance the fraction at the output of CF 1, which were due to current flow through the micro-electrode alone.

The current-generating equipment on the left side of Fig. 1 was 'locked' to the sweep through a square-wave generator driving a Carpenter high-speed relay (Type 3 GI). The polarizing unit (POL) isolated from earth, provided voltages of 0–45 V of either polarity and was connected via a length of shielded cable to the micro-electrode by a resistance of 100 or 500 MΩ. This enabled current to be passed into the motoneurone through either a single electrode or one side of a double electrode and at the same time ensured that there was minimal distortion in the recording of potential changes arising from responses of the cell. The current flowing in this circuit was measured as the potential drop across a resistance of 1 MΩ to earth. After amplification by AMP. E–DC, it was displayed on the lower beam of CRT 2. The appropriate bridge network was linked to the polarizing unit through a cathode follower (CF 2) so that the current measured by AMP. E was predominantly that flowing in the micro-electrode circuit. The network was then connected through another cathode follower input stage (CF 3) to the other side of the differential amplifier. In more recent experiments, rectangular pulses of current have been applied by means of a series of radio-frequency isolation units (Grass SIU 4). In this fashion polarizing units providing rectangular voltage pulses need not be isolated from earth and it was possible to use briefer

pulses than those obtained by means of a relay. A further modification was made in the method of recording the current passing through the electrode. The voltage developed across a resistance of 10 MΩ, connected between the electrode and the 100 or 500 MΩ resistance in the current-carrying line, has been measured by means of a DC amplifier having a differential input.

The equivalent circuit for a single electrode and a motoneurone is represented in Fig. 2*A*. The effective input capacity of CF 1, with an attached micro-electrode penetrating 3 mm into the spinal cord, is $5–10 \times 10^{-12}$ F. It is obviously impracticable to make a network using these values of capacity, but as it was essential to reproduce potentials at CF 3 with the same intensity and time course as those at CF 1, the network was made with capacities one hundred times greater than those of the micro-electrode system and resistances one hundredth of the corresponding values. All components of the network were made readily adjustable in order to match capacities

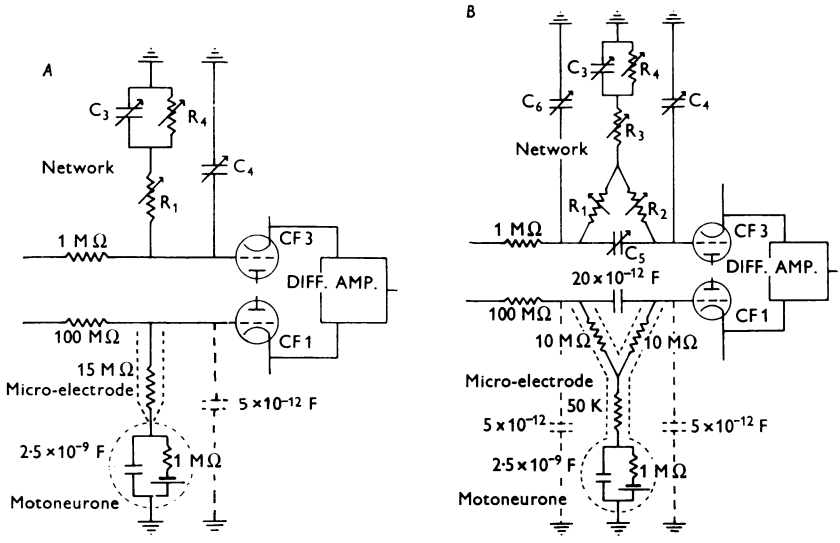

Fig. 2*A*. Circuit showing the network used for producing compensating artifacts when recording with a single micro-electrode.

Fig. 2*B*. Circuit showing the network used for producing compensating artifacts when recording with double micro-electrodes.

and resistances that had considerable variation. A comparable circuit was used for double micro-electrodes (Fig. 2*B*). The capacitive coupling of about 20×10^{-12} F between the current passing and the recording barrel makes it impossible without compensation to follow potential changes over the first 2–3 msec after the onset of a pulse (Coombs *et al.* 1955), but with the circuit of Fig. 2*B* this artifact could be balanced out. With the micro-electrode tip in an extracellular position, under ideal circumstances it would be possible to adjust R_1 and C_4 in Fig. 2*A* and R_1, R_2, R_3, C_4, C_5 and C_6 in Fig. 2*B* until an applied current pulse produced no voltage change at the output of the differential amplifier. Then, when a neurone was impaled, all the potential change during an applied current pulse would be due to the passage of the pulse through its membrane. However, when the electrode was in an extracellular position or even with its tip in 0·9 % NaCl solution, it frequently did not behave as a simple resistance. This was particularly obvious with currents greater than 30×10^{-9} A and with electrodes having resistances in excess of 20 MΩ. The usual finding was that resistance increased as the current increased. Furthermore, with the single electrode, reversal of the current pulses sometimes did not produce a mirror-image change in the recorded potential, as reported by Araki & Otani (1955). This distortion was usually negligible with double electrodes,

presumably because the recording barrel and the current-passing barrel are virtually independent, sharing only the relatively low coupling resistance. It appears therefore that the micro-electrodes change their electrical properties during the passage of current (cf. Jenerick & Gerard, 1953; Frank & Fuortes, 1956). Such an effect could be expected to arise because of both the ionic migration caused by the current and the interaction of ions with the glass surface at the most constricted part of the micro-electrode (del Castillo & Katz, 1955; Weidmann, 1955; Adrian, 1956). Consequently, on account of the non-linear behaviour of the electrodes and also because the resistance of an electrode fluctuates considerably as it passes through the spinal cord, especially when the tip is advancing, the best approximation that usually could be made was to record the potentials produced by currents applied in both directions intracellularly, with approximate conditions for balance of the electrode by the network, and then to repeat the observations immediately after withdrawal of the electrode from the motoneurone. The differences between the two series of potential curves were assumed to be due to potentials across the motoneuronal membrane. In practice the rising phase of the current was distorted by the capacity C 2 (Fig. 1) of the current-passing line. However, the time constant of the rise of the pulse was rarely greater than 100 μsec, which is small when compared with the membrane time constant. In Fig. 1 the variable capacitor C 1 was used in compensating for the capacitance C 2 between the current-passing line and earth. The current pulse through the electrode being rectangular, C 1 was adjusted until the potential recorded across the resistance of 1 MΩ was not only rectangular, but equivalent in size to that recorded when an equivalent constant current was flowing.

For double electrodes the ancillary equipment was considerably more complex than that for a single one. The addition of a switch allowed either barrel to be used for recording or for passing current. Consequently, the capacitor C 6 (Fig. 2*B*) was used to compensate for the extra capacitance to ground on the current-passing side of the electrode. This value was rarely greater than 5×10^{-12} F and C 6 was often omitted.

These circuits were tested using an artificial network to replace the micro-electrode and the cell. Provided compensation was reasonable with circuits equivalent to an extracellular position of the micro-electrode tip, the potentials recorded when a 'cell' was added had the time courses and magnitudes that would be expected from the electrical properties of the circuit representing the cell.

RESULTS

Resistance of motoneuronal membrane

Measurement of membrane resistance. The most direct method of determining the membrane resistance of motoneurones is to measure the potentials produced by the passage of known currents across the membrane, as was first done by Coombs *et al.* (1955), employing for this purpose a double micro-electrode, one barrel for current and the other for potential measurement. In this earlier work the current was usually allowed to flow for several seconds before the potential measurements were made, but briefer current pulses gave approximately the same results.

Essentially the same method has been employed in the present investigation, but compensation for potentials produced by extraneous factors of capacity and resistance has allowed an accurate record to be made of the time course of the potential change across the motoneuronal membrane. For example, in Fig. 3 the difference between the potential curves obtained inside and outside the motoneurone for a given rectangular current pulse gives the potential change across the soma membrane of the motoneurone. The

extracellular records of L and M show that, except for the brief transients, the adjustment of the compensatory circuit had virtually eliminated all potential changes apart from those due to the motoneurone membrane. Furthermore, the intracellular potential changes produced by depolarizing (J) and hyperpolarizing (K) currents were almost mirror images.

The final plateau potential was directly proportional to the current intensity, as is shown by the straight line through the dots of Fig. 4. Actually the plotted potentials in Fig. 4 are corrected for the small extracellular plateau potentials of L and M, and are shown relative to the resting membrane potential of -69 mV at zero current. This linear relationship of potential to current has been regularly observed, there being usually no appreciable rectification

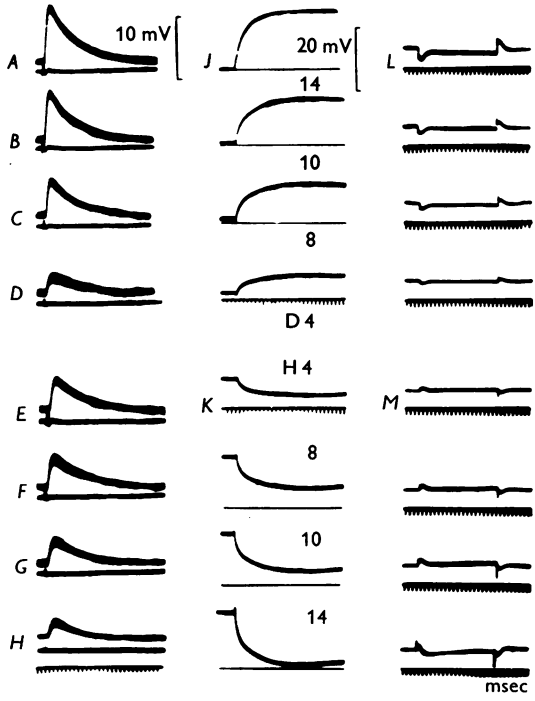

Fig. 3. Intracellular recording (double-barrel K_2SO_4 micro-electrode) from a lateral gastrocnemius motoneurone (resting membrane potential, -69 mV) showing EPSP's produced by Group Ia volleys from lateral (A–D) and medial gastrocnemius nerves (E–H). In addition, the spike potentials of the afferent volleys, as recorded by an electrode on the appropriate dorsal root, show that the Group Ia volleys were submaximal in C–F. All records are formed by the superposition of about 40 faint traces. J and K show intracellular potential changes for depolarizing and hyperpolarizing pulses with strengths indicated in units of 10^{-9} A, the artifacts being largely balanced out by the compensatory circuit of Fig. 2B. L and M show just-extracellular potential changes for these same current pulses and the same setting of the compensatory circuit. Note separate potential scales for the synaptic potentials and the pulse responses. Time scales are shown throughout in milliseconds.

due to a lower resistance to hyperpolarizing currents, as previously reported (Coombs *et al.* 1955). The slope of Fig. 4 corresponds to a membrane resistance of 1·0 MΩ. Resistances measured in this way from the directly determined current:voltage relationship for some motoneurones are shown in column 5 of Table 1. Altogether, reliable measurements have been obtained for twenty-seven motoneurones in good conditions, the range being 0·6–2·5 MΩ with a mean value of 1·2 MΩ.

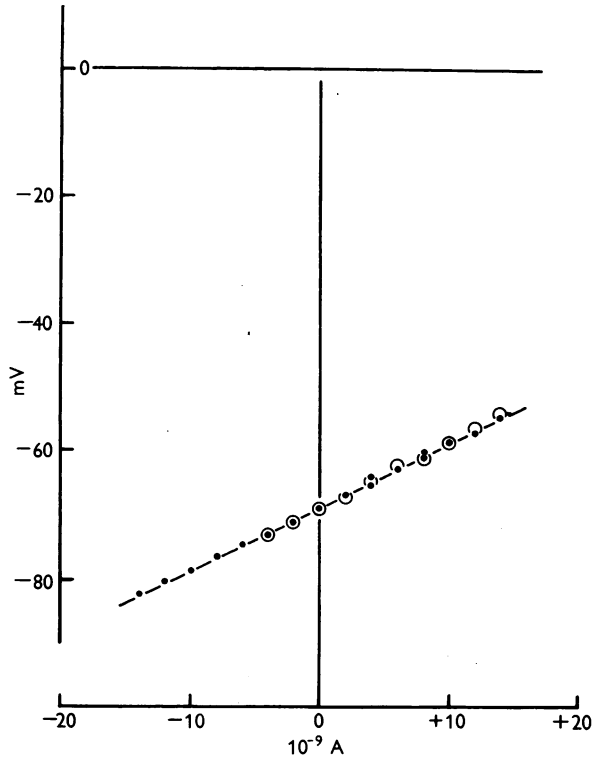

Fig. 4. For each strength of polarizing current the final membrane potential is determined by subtracting the extracellular from the intracellular records for the series partly illustrated in Fig. 3 *J–M*. The dots show that the points so obtained lie on a straight line with a slope corresponding to 1·0 MΩ. With the open circles the membrane potential has been determined on the assumption that the membrane potential at the spike summit is unaltered by the polarizing current (see text).

Many micro-electrodes were defective in passing currents, exhibiting both a rectification and a progressively increasing resistance with the continued passage of currents (cf. Frank & Fuortes, 1956). These defects are attributable to electrode polarization (cf. Adrian, 1956) and are readily recognized with the micro-electrode in an extracellular position. Intracellular observations with such electrodes have been rejected. As would be expected, electrode polarization

has been much more troublesome when a single micro-electrode has been employed both for the current and for potential measurement, and almost all the resistances have been measured with double electrodes (cf. Table 1).

TABLE 1. Measurements of resistance of motoneuronal membrane

				Membrane resistance measurements (MΩ)			
						Spike method	
Experiment	Electrode type	Cell type	Membrane potential (mV)	Direct method	Threshold method	Anti-dromic	Ortho-dromic
1	2	3	4	5	6	7	8
18/1/56	*S* K_2SO_4	Pl	−66	1·0	—	—	—
16/2/56	*S* K_2SO_4	Pl	−68	0·8	—	—	—
16/2/56		GS	−60	2·5	—	—	—
28/2/56		?	−65	2·0	—	—	—
20/6/56		BST	−55	1·3	—	—	—
25/6/56		GS	−68	1·0	—	—	—
25/6/56		GS	−62	0·8	—	—	—
25/6/56		BST	−60	0·8	—	—	—
25/6/56		BST	−60	1·2	—	—	—
18/7/56		BST	−65	1·2	—	—	—
20/11/56	*D* K_2SO_4	Pl	−70	—	1·1	1·3	1·4
20/11/56		SM	−71	1·4	—	—	—
1/2/57		BST	−56	1·0	—	—	—
1/2/57		BST	−57	1·2	—	—	—
1/2/57		GS	−64	0·6	—	—	—
1/2/57		GS	−63	0·7	0·7	0·2	—
1/2/57		BST	−56	1·0	1·0	0·6	—
1/2/57		FDL	−60	1·4	—	—	—
5/2/57	*S* KCl	BST	−60	1·8	—	—	—
5/2/57		MG	−63	1·6	—	—	—
5/2/57		LG	−69	1·0	0·7	0·8	—
5/2/57	*D* K_2SO_4	BST	−66	0·6	—	—	—
5/2/57		MG	−50	1·2	—	—	—
28/4/57		BST	−66	—	0·95	0·93	0·95
7/5/57		FDL	−68	—	0·65	0·7	—
29/5/58	*S* K_2SO_4	BST	−72	0·6	—	0·62	—
29/5/58	*S* K_2SO_4	BST	−63	0·5	—	0·55	—
11/6/58	*S* KCl	?	−74	1·4	—	1·1	—
Means			−64	1·15			

In this and subsequent tables the cell species are as follows:

BST = biceps semitendinosus; GS = gastrocnemius-soleus; FDL = flexor digitorum longus; Pl = plantaris; MG = medial gastrocnemius; LG = lateral gastrocnemius; SM = semimembranosus; S = soleus; Per = peroneal. *S* = single, *D* = double.

As a consequence of these polarization difficulties with single micro-electrodes, Frank & Fuortes (1956) introduced two more indirect methods of measuring the change of membrane potential produced by current. However, it should be noted that Araki & Otani (1955) and Ito (1957) measured membrane resistances to current flowing through a single micro-electrode, employing a compensatory circuit to balance out potentials arising in the electrode. Apparently they were not seriously troubled by electrode polarization.

The first method depends on the assumption that there is the same threshold level of depolarization for initiating a spike, regardless of the proportion con-

tributed by current directly applied or by excitatory synapses (cf. Frank & Fuortes, 1956; Coombs, Curtis & Eccles, 1957). Thus the depolarization produced by any applied current can be measured simply by subtracting the threshold level for superimposed EPSP from the threshold level for the EPSP in the absence of current. When the depolarizations are calculated in this way for different strengths of applied currents, there is found to be an approximate proportionality between potential and current, the proportionality constant giving a measure of the membrane resistance. Records obtained in this type of experimental procedure have already been published (Frank & Fuortes, 1956, Fig. 2; Coombs *et al.* 1957, Figs. 6, 11), and the membrane resistances so measured in the present investigation are shown in Table 1, column 6.

The second indirect method of measuring membrane resistance (Frank & Fuortes, 1956) depends on the assumption that the passage of relatively small currents across the motoneuronal membrane does not alter appreciably the membrane potential at the spike summit. This assumption is based on an analogy with the spikes in squid giant axons, frog muscle fibres, and the supramedullary neurones of the puffer fish, where the membrane resistance at the peak of the spike is less than 5% of the resting value (Hodgkin & Huxley, 1952; Fatt & Katz, 1951; Hagiwara & Saito, 1957), and where the ionic mechanism generating the spike is little, if at all, affected by the flow of current across the membrane. Thus, as a first approximation, the changes produced in spike heights by the passage of hyperpolarizing and depolarizing currents across the membrane may be used as a measure of the changes produced in the resting membrane potential, and hence for determining the resting membrane resistance. For example, the open circles of Fig. 4 were derived in this manner for the motoneurone illustrated in Fig. 3. The virtual identity of the slopes of the straight lines through the dots and open circles in Fig. 4 shows that the indirect and direct methods give the same value for the membrane resistance. However, in some motoneurones (cf. Table 1, column 7), there was a considerable discrepancy between the direct and the second indirect method.

A defect in this indirect method arises on account of the alteration of the delay between the two components (IS and SD) of the spike potential (cf. Coombs *et al.* 1955, Fig. 7; Coombs *et al.* 1957, Figs. 10, 11). With antidromic spike potentials, in particular, a depolarizing current shortens the IS–SD delay, but a hyperpolarizing current lengthens it. Thus with depolarizing currents there is a closer approximation to synchronism and hence the spike potential would be less diminished than would be expected from the change actually produced in the membrane potential. Conversely, with hyperpolarizing currents the increasing asynchronism would cause the spike potential to be increased by less than the change produced in the membrane potential. This change in asynchronism is much less with spikes generated by synaptic stimulation (cf. Frank & Fuortes, 1956, Fig. 2; Coombs *et al.* 1957, Figs. 10, 11), which therefore is the method of choice, but only two neurones have been measured in this way (Table 1, column 8). It will be appreciated that this effect of changing IS–SD delay will cause the membrane resistance to be underestimated. Furthermore, there should be a small addition to these indirect measurements (about 5%) in order to allow for the small resistance that the membrane still has at the spike summit.

The interpretation of resistance measurements. All the above methods of measuring the membrane resistance of motoneurones have been based on the potential changes that are produced when currents are passed into them by means of an intracellular micro-electrode. Unfortunately, the motoneurone has not a simple geometrical configuration, so specific resistance of the motoneuronal membrane can be calculated only after the distribution of current flow has been derived from an assumed standard structure of the motoneurone. The values given by Coombs *et al.* (1955) were, in fact, derived in this way, but more detail will now be given, because an alternative derivation has been proposed (Rall, 1957). According to Balthasar (1952) the motoneurones in the cat lumbar enlargement have on the average about 6 dendrites. From Balthasar's account and from our own unpublished observations the standard motoneurone may be regarded, in the first approximation, as being a sphere 70μ in diameter from which arise seven processes (six dendrites and one axon). The dendrites usually have a conical origin, but soon become fairly uniform cylinders about 5μ in diameter that branch relatively infrequently until they are several hundred microns from the parent cell. For present purposes the dendrites may be regarded as indefinitely extended cylinders, because it will emerge from the calculations that this terminal branching is at least one to two length constants removed from the soma, and hence would be relatively little influenced by currents applied within the soma by a micro-electrode.

If a current is applied to the interior of one end of an indefinitely extended uniform cylinder surrounded by a membrane having a resistance of $r_m \times$ unit length and immersed in a volume conductor, the effective resistance of the cylinder is $(r_m r_i)^{\frac{1}{2}}$, where r_i is the resistance of unit length of the core (Hodgkin & Rushton, 1946; Fatt & Katz, 1951). Assuming the cylinder diameter to be 5μ and the specific resistivity of the core to be $75\,\Omega.\text{cm}$, which corresponds approximately to its ionic composition, $r_i = 3{\cdot}8 \times 10^8\,\Omega/\text{cm}$, and $r_m = 6{\cdot}4 \times 10^2\ R_m\,\Omega.\text{cm}$, where R_m is the specific resistivity of the surface membrane. Thus the resistance of one dendrite as measured by the application of current to the soma (as in the experiments) would be $4{\cdot}9\ R_m^{\frac{1}{2}} \times 10^5\,\Omega$, and for seven such processes (assuming the axon to be equivalent to a dendrite) the resistance, R_D would be $7\ R_m^{\frac{1}{2}} \times 10^4\,\Omega$. If the surface membrane of the soma (a sphere 70μ in diameter) be assumed to have the same specific resistivity, R_m, its resistance, R_S, as measured by the intrasomatic application of a current would be simply $6{\cdot}5\ R_m \times 10^3\,\Omega$, since all parts of the approximately spherical soma membrane would be passing the current uniformly (Rall, 1955). In the experimental situation the soma and dendrites are resistances in parallel, hence, if the total measured resistance is R_{SD},

$$1/R_{SD} = 1/R_S + 1/R_D,$$

where $$R_S = 6{\cdot}5\ R_m \times 10^3\,\Omega \text{ and } R_D = 7\ R_m^{\frac{1}{2}} \times 10^4\,\Omega.$$

Values of R_m may thus be simply calculated from this quadratic equation for various values of R_{SD} and hence the corresponding values for R_S and R_D may be obtained. Table 2 gives these values for four measurements of R_{SD}, which cover almost the whole range of the experimental determinations, the one at 1·2 MΩ representing the mean value (cf. Table 2, column 5).

Measurement of the electric time constant by the effects produced by a rectangular current

Membrane potential change. In addition to giving the final levels of the potential changes produced by various currents, Fig. 3 allows the time courses to be determined by subtracting the extracellular from the corresponding intracellular records (*L* from *J* and *M* from *K*). The potential curves so derived deviate from the exponential form expected for the conventional

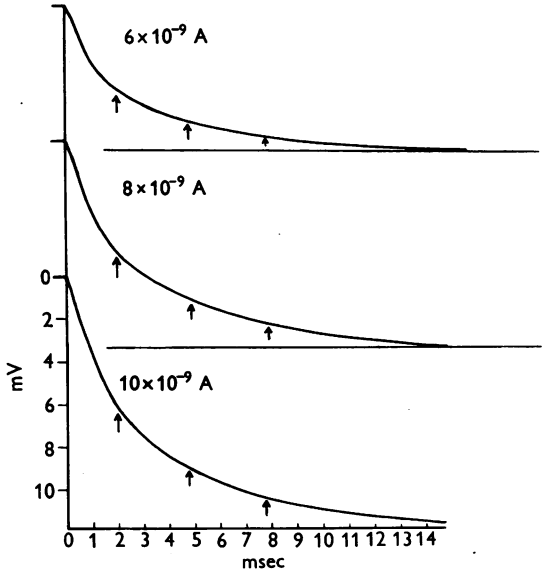

Fig. 5. The time course of the membrane potential change produced by current pulses in Fig. 3 has been determined by subtracting the extracellular from the corresponding intracellular curve and averaging the depolarizing and hyperpolarizing potentials (neglecting the opposite sign) at each of the three current strengths shown. The arrows mark the succesive half-times of the curves beginning at 2 msec after the start of the pulses, by which time the initial artifacts will be negligible.

equivalent circuit for the membrane, i.e. for a resistance and capacitance in parallel. As is shown in Fig. 5 there is a progressive lengthening of the successive half-times in the curves derived from the experimental records illustrated in Fig. 3.

The decay of the membrane potential on cessation of the rectangular pulse of current followed an identical time course. However, when the pulses were

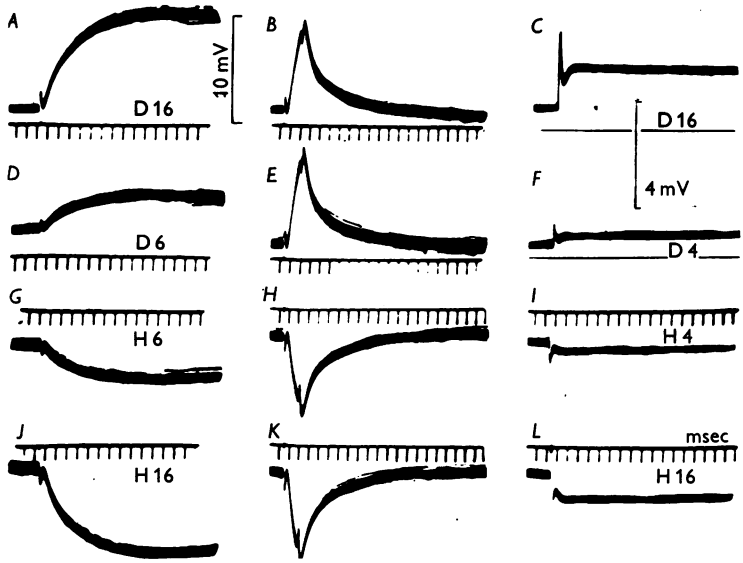

Fig. 6. *A*, *D*, *G*, *J* show records from a gastrocnemius motoneurone with a resting membrane potential of −70 mV, the current strengths being indicated in units of 10^{-9} A. In *B*, *E*, *H*, *K* the current pulses were only 1·5 msec in duration, the respective strengths being 47, 51, 55 and 61×10^{-9} A, in the depolarizing and hyperpolarizing directions respectively. *C*, *F*, *I* and *L* are extracellular records with the same setting of the compensatory circuit, the respective pulse strengths being indicated in units of 10^{-9} A.

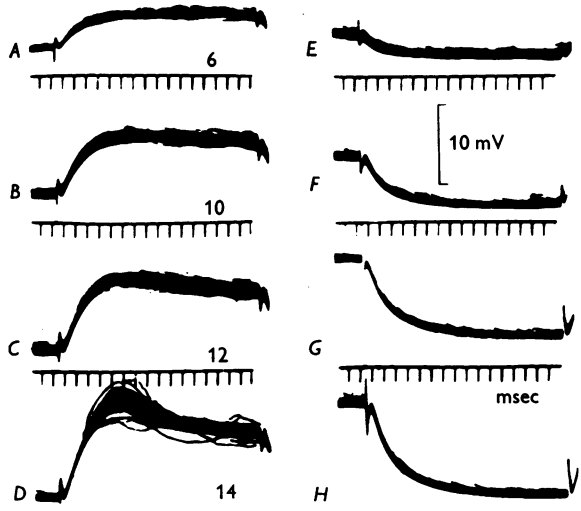

Fig. 7. Intracellular records with a double K_2SO_4 electrode from a biceps-semitendinosus motoneurone, the resting membrane potential being −50 mV. Current pulses in the depolarizing (*A–D*) and hyperpolarizing directions (*E–H*) were applied as in Fig. 3 *J*, *K*, the current strength being indicated in units of 10^{-9} A. All records are formed by the superposition of about 40 faint traces, and the initial artifact is minimized by the compensatory circuit of Fig. 2*B*.

brief as in Fig. 6*B*, *E*, *H*, *K*, the initial phase of decay was much faster. When half-times were measured from 1 msec after cessation of current, values as brief as 1·3 msec were obtained, in contrast to 1·6 msec for the equivalent half-times following the onset of the long current pulse in *A*, *D*, *G*, *J*. The explanation of this discrepancy will appear when considering the distribution of current flow in the soma and dendrites of the motoneurone.

In some motoneurones local responses caused hump-like additions to the potential changes produced by depolarizing currents. These humps are obvious in Fig. 7*D*, but presumably are also responsible for causing the depolarizing responses in *B* and *C* to run a faster time course than the corresponding hyperpolarizing responses (*F* and *G*). Local responses as prominent as those of Fig. 7 are usually exhibited only by deteriorated motoneurones, and are also a feature of chromatolysed motoneurones (Eccles, Libet & Young, 1958). Nevertheless, with very weak currents there is approximate symmetry between depolarizing and hyperpolarizing responses, as in Fig. 7*A*, *E*, so reliable values may still be obtained for the time courses of the passive membrane changes.

Rall (1957) has provided a theoretical treatment in which the time course of the potential recorded within the soma is considered in relation both to the distribution of current between the dendrites and soma and to the membrane time constant, which is assumed to be the same for dendrites and soma. On the basis of the very high value of $2000\,\Omega.\mathrm{cm}^2$ which he assumes for the specific membrane resistance, he calculates that, at the steady state, about 5 times as much current passes through the dendritic membrane as through the soma membrane. Given the same anatomical structure and the mean resistance of 1·2 MΩ as measured by an electrode in the soma (Table 1, column 4), a much lower value can be calculated for the specific membrane resistance (about $600\,\Omega.\mathrm{cm}^2$ in Table 2) and the dendritic current is then only 2·3 times the soma current (Table 2). Consequently, the observed time course for soma membrane potential would be considerably less distorted than in the condition calculated by Rall.

Figure 8 shows the curves calculated by Rall for the approach to a steady membrane potential when a constant current is applied through an intrasomatic electrode at zero time. The lower and upper broken lines give respectively the time course for a soma without dendrites and for dendrites without soma. The former curve is, of course, a strictly exponential curve approaching to $(1-1/e)$ of its final value in a time equal to the time constant of the membrane. The dotted line gives the time course of potential change for the conditions assumed by Rall with a ratio of 5:1 for dendrite:soma current flow at the steady state. The continuous line gives approximately the time course of potential change when that ratio is 2·3:1, which is derived in Table 2 for the assumed standard configuration of the motoneurone and for the mean

intrasomatic resistance, 1·2 MΩ. Rall suggested that the membrane time constant could be derived from the soma–dendrite curve (the dotted line of Fig. 8) by observing the time for attainment of 82% of the final value, which would be about 76% when a ratio of 2·3 was substituted for 5. Unfortunately, this method could not be applied because, in spite of the bridge network used to compensate for the properties of the electrode, it was impossible in most cases to study the first one or two milliseconds of the potential changes generated by current pulses. It was necessary, therefore, to employ an alternative

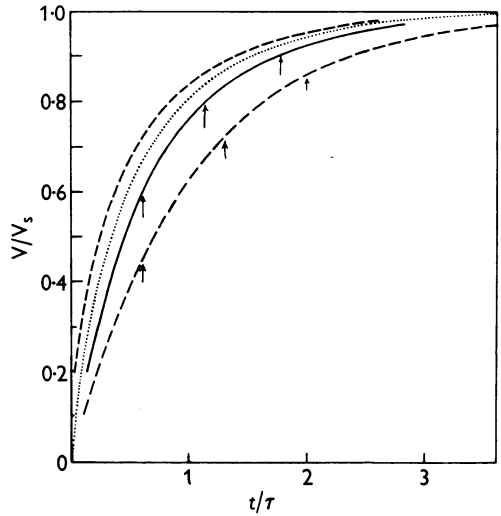

Fig. 8. Diagram, modified from Rall (1957), to show the calculated time courses of potential changes produced by the application of a constant applied current to various relationships of the dendrites and soma of a motoneurone. The time scale is measured relative to the membrane time constant, τ, which is assumed to be uniform over the soma and dendrites. The lower broken line is for soma without dendrites, the upper for dendrites without soma, and the two intermediate curves are for various combinations of soma and dendrites. The dotted line is the curve calculated by Rall on the basis of a steady dendrite current five times the soma current. The continuous line represents approximately the curve if, as is here assumed, the ratio of dendritic to soma current is only 2·3. The arrows show the successive half-times, commencing at $t = 0{\cdot}6\tau$.

TABLE 2. Calculations relating to soma and dendrite resistance for a standard motoneurone with six dendrites

Measured resistance by intrasomatic electrode, R_{SD}(MΩ)	Calculated specific membrane resistance, R_m(Ω.cm²)	Calculated soma resistance, R_S(MΩ)	Calculated dendrite resistance, R_D(MΩ)	Ratio, $R_S : R_D$	Effective surface area of motoneurone (cm²)	Length constant of dendrite, λ; $(r_m/r_l)^{\frac{1}{2}}$ (μ)
1	2	3	4	5	6	7
0·5	172	1·06	0·92	1·15	$3{\cdot}4 \times 10^{-4}$	170
1·0	470	3·05	1·50	2·03	$4{\cdot}7 \times 10^{-4}$	280
1·2	615	4·0	1·74	2·30	$5{\cdot}1 \times 10^{-4}$	322
2·0	1390	9·0	2·6	3·45	$6{\cdot}9 \times 10^{-4}$	485

procedure in which the two successive half-times were measured after this initial distorted phase. For example, such measurements would be made for the continuous curve of Fig. 8 between the three arrows, and in Fig. 5 the arrows are likewise shown for experimental curves. The half-time for the soma curve of Fig. 8 (the lower broken line) is found to be 1·2 times the mean half-time thus derived from the assumed soma–dendrite curve. Thus the approximate membrane time constant for the motoneuronal membrane has been derived from curves such as those illustrated in Fig. 5 by finding the mean half-time and then multiplying by $1{\cdot}2 \times 1{\cdot}43$. The values shown in Table 3, column 5,

TABLE 3. Measurements of electric time constant of motoneuronal membrane

				Time constants (msec)			
Experiment 1	Electrode type 2	Cell type 3	Membrane potential (mV) 4	Derived from potential changes 5	Strength–latency measurement 6	Anti-dromic block method 7	Direct pulse measurements 8
1/12/55	*S* KCl	BST	−70	2·4	1·2	1·1	—
4/1/56	*S* K_2SO_4	BST	−70	2·0	0·75	—	—
28/2/56	*S* KCl	?	−65	4·2	—	2·2	—
20/6/56		?	−60	2·6	1·1	—	—
20/11/56		Per	−75	4·9	1·35	2·3	—
20/11/56		SM	−71	1·8	—	1·1	—
1/2/57		GS	−64	2·5	0·6	—	—
1/2/57		?	−65	1·8	0·75	—	—
1/2/57	*D* K_2SO_4	GS	−66	3·1	1·4	—	—
1/2/57		BST	−58	3·6	0·9	—	—
1/2/57		FDL	−60	3·0	1·3	—	—
5/2/57		MG	−60	3·9	1·3	—	—
5/2/57		S	−54	2·8	1·4	—	—
5/2/57		LG	−69	5·1	1·0	—	—
5/2/57		BST	−66	3·6	1·1	—	—
29/5/58	*S* K_2SO_4	Pl	−81	2·4	0·92	—	2·45
29/5/58	*S* K_2SO_4	BST	−72	2·6	0·92	—	—
11/6/58	*S* KCl	?	−70	4·2	1·6	—	—
Means	—	—	−66	3·1	1·1	—	—

were measured in this way, and consequently can be regarded as being only very approximate, depending as they do on so many assumptions of doubtful validity. The progressive electrotonic distribution of potential from soma to dendrites accounts not only for the deviation of the rising phase of the potential curves from the exponential form, but it also accounts for the faster decay of potentials set up by brief pulses, as in Fig. 6 *B*, *E*, *H*, *K*. Under such conditions the potential change will not be so effectively distributed along the dendrites.

Strength–latency relationship. Frank & Fuortes (1956) derived the membrane time constant from the curve expressing the relationship between intensity of rectangular pulses and the latency of spike initiation. If the current is applied uniformly to the whole excitable membrane, the potential will rise exponentially to its steady-state value, and, assuming that the threshold for

spike initiation is independent of the rate of rise, that is, that accommodation is negligible,

$$I_{rh}/I = 1 - e^{-t/\tau},$$

where I is the current which stimulates in time t; I_{rh} is the rheobasic current and τ the membrane time constant. From this equation it follows that when $t=\tau$, $I=1{\cdot}58\ I_{rh}$. Thus, in a series such as that illustrated in Fig. 9 and plotted in Fig. 10, the points lie on a curve which shows that a current 1·58 times rheobasic strength stimulates with a latency of 0·92 msec, i.e. a value of 0·92 msec is derived for τ, the membrane time constant. The time course of the membrane potential changes directly observed in this same motoneurone are plotted in the inset of Fig. 10 for a series of currents in both depolarizing and hyperpolarizing directions, and extracellular recording showed that the compensation had effectively neutralized all potential changes after 1 msec. When measured after 1 msec from the onset of the current pulse, the mean values of the two successive half-times were 1·45 and 1·6 msec respectively. Evidently there is a large discrepancy between the membrane time constant of 0·92 msec derived from the strength–latency curve and one of 2·2 msec derivable from the observed changes in membrane potential, and which should be still larger when allowance is made for the dendritic distortion, when the value for τ would be about 2·6 msec. Discrepancies of this order are shown in Table 3, columns 5 and 6, for every motoneurone in which both measurements have been made, and lesser discrepancies in the same direction were reported by Frank & Fuortes (1956).

Considerable disabilities are associated with the use of strength–latency curves in determining the time constant of the motoneuronal membrane. In the first place the equation is based on the assumption that rectangular current pulses evoke membrane potential changes that approach exponentially the steady-state value with a time constant characteristic of the membrane. The distortion due to dendritic current flow will cause the derived time constant to be much below that actually obtaining for the membrane. A further major disability is that the applied current is not the only means by which the membrane is being depolarized. Local responses will provide active depolarization as the threshold is approached, and the background synaptic bombardment by excitatory impulses (synaptic noise, cf. Brock, Coombs & Eccles, 1952) will tend to shorten the latency for any particular current. Finally, accommodation provides a distortion which is difficult to assess, and which appears to vary considerably with different motoneurones. All these distortions will tend to diminish the value of τ derived from strength–latency curves. The large discrepancies exhibited in Table 3, columns 5 and 6, thus seem to be adequately explained.

As would be expected on account of these various distorting factors, the strength–latency curves deviate systematically from the curve derived from the

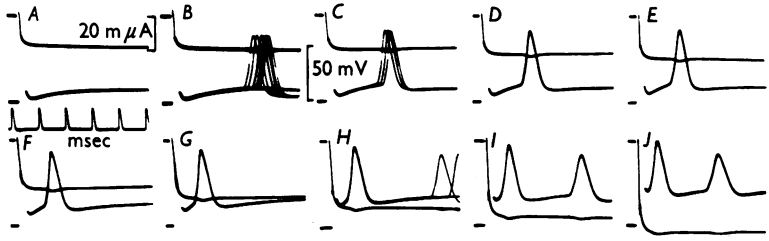

Fig. 9. Lower traces show intracellular potential changes produced in a biceps-semitendinosus motoneurone by current pulses progressively increased from *A*–*J* and applied through one barrel of a double micro-electrode (K_2SO_4), the artifacts being minimized by the compensatory circuit of Fig. 2*B*. Resting membrane potential, −69 mV. All records are formed by the superposition of several traces at one-second intervals. Upper traces (with downward deflexion) signal the current pulses, the scale being shown in 10^{-9} A. Note that in *G*–*I* in particular there is superposition of the current and potential traces. The artifact at the beginning of the potential trace has been deleted in order to avoid confusion of the traces. Time in msec for all records. Current in *B* is at rheobasic strength and in *A* it is below the rheobase.

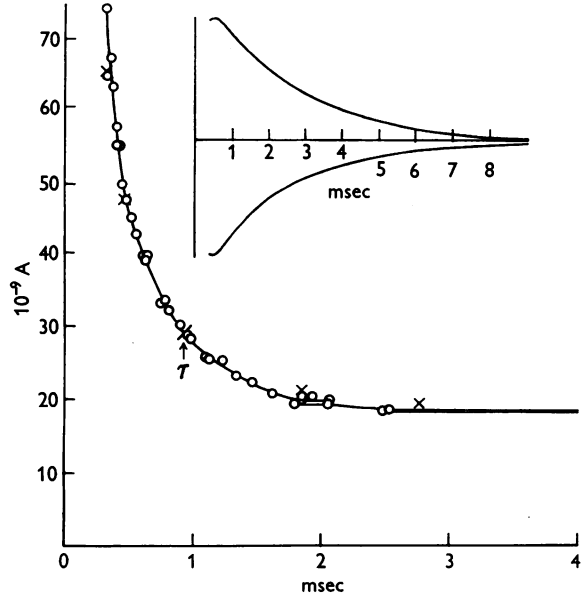

Fig. 10. The open circles plot the strength of current against the latency for spike initiation for the series partly shown in Fig. 9. At strengths close to rheobase, horizontal lines join points showing shortest and longest observed latencies (cf. Fig. 9*B*, *C*). The value of the membrane time constant as so derived is shown by the arrow giving latency for a current 1·58 times rheobasic strength. The oblique crosses give points on the theoretical curve (see text). The inset curves give the time course of the membrane potential changes produced by depolarizing and hyperpolarizing current pulses of 10×10^{-9} A that commence at zero time.

equation. For example, if the theoretical curve in Fig. 10 (the oblique crosses are on this curve) is adjusted so that it passes through the strength–latency curve at a point 1·58 times rheobasic strength, i.e. with $t=\tau$, the observed latencies are longer than predicted for all stronger strengths, and briefer for all weaker strengths.

The time course of excitability. When a rectangular current pulse is applied to a motoneurone, the time course of the change in membrane potential may also be measured by applying a brief testing stimulus. The most satisfactory procedure is that introduced by Frank & Fuortes (1956). A testing pulse with a constant duration of not more than 0·3 msec is superimposed at various times during and after the rectangular pulse, and for each position the intensity is

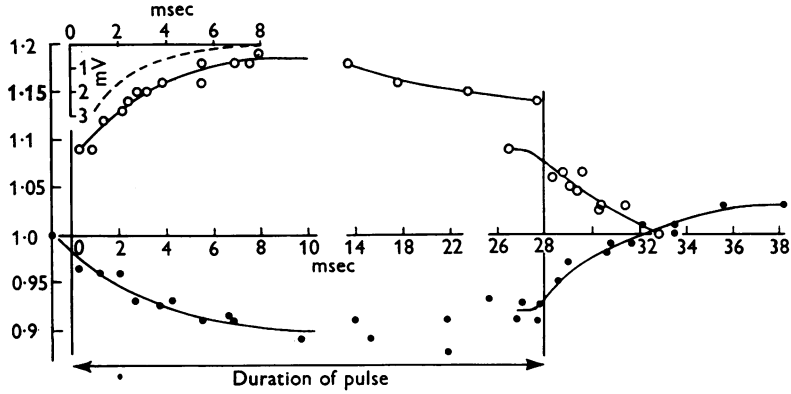

Fig. 11. Excitability changes produced in a plantaris motoneurone by application of small hyperpolarizing (open circles) and depolarizing (filled circles) current pulses of 28 msec duration. Double K_2SO_4 electrode. Resting membrane potential, −81 mV. Each point represents the strength of a testing pulse of 0·3 msec duration that was required to generate an impulse in about 50 % of the trials when superimposed at the indicated intervals in relationship to the conditioning pulse. The testing pulse strength is shown relative to the control strength which was determined at frequent intervals and which remained virtually constant throughout the whole series. Initially the hyperpolarizing pulse was 4×10^{-9} A, but with the point just before and those after the cessation of the pulse the strength was inadvertently reduced to $2{\cdot}5 \times 10^{-9}$ A. The depolarizing current was at this reduced strength throughout the whole series. Note change in time scale from 10 to 26 msec. Inset curve (broken line) shows time course of membrane potential change produced by the current pulse. It is the mean of the depolarizing and hyperpolarizing potentials as in Fig. 5.

determined that excites an impulse in approximately 50 % of the trials. The threshold intensities of the testing stimuli can be expressed as fractions of the control threshold intensity, that is, in the absence of the rectangular pulse, and plotted against the temporal position of the test as in Fig. 11. When the rectangular pulses in the depolarizing and hyperpolarizing directions were relatively weak, the excitability curves so determined were approximately mirror images, just as was observed with the membrane potentials produced by the current pulses (Figs. 3, 5). If accommodation is negligible, these

excitability curves should express the time course of the change in membrane potential produced by the rectangular current (cf. inset figure with broken line in Fig. 11) and good agreement is observed in these two time courses in Fig. 11. Frank & Fuortes (1956) found a small amount of accommodation in the three motoneurones that were tested during long depolarizing currents (100 msec). A similar accommodation is seen in Fig. 11 from 14 to 28 msec during a hyperpolarizing current and is also indicated for the depolarizing current, at least during the latter part of this period.

On cessation of long rectangular currents the excitability shows the reverse change with a comparable time course after 28 msec in Fig. 11, but tends to overshoot, as would be expected for the accommodation reaction. Thus the membrane excitability exhibits a rather faster time course than the membrane potential. This procedure has been tried on several motoneurones, but, on account of spontaneous variations in excitability, a reliable value for the time constant was obtained only in the example illustrated (cf. Table 3, column 8), where it is seen to be in good agreement with the value in column 5.

Less satisfactory procedures for measuring the time course of the excitability change employ as tests either antidromic or orthodromic stimulation of the motoneurone. In the usual procedure the intensity of the rectangular pulse was varied, so that at each testing position a spike was evoked in 50% of the trials. For example, the depression of excitability by a rectangular hyperpolarizing current can be tested by its power of blocking the antidromic invasion of a motoneurone. In this way a curve is obtained relating current strength to the time at which a certain depression of excitability is attained. Similarly, the increase in excitability produced by a rectangular depolarizing current could be tested by a fixed subthreshold synaptic stimulus, or by an antidromic impulse that normally failed to invade the soma of the motoneurone. The curves are of the same form as those discussed above in relation to the strength–latency measurements, and, if it be assumed that the time courses of the excitability changes on the membrane are of an exponential nature, the same formula can be applied. Thus when $t=\tau$, $I=1{\cdot}58\,I_{rh}$, where I is the current used and I_{rh} the rheobasic current producing the phenomena under observation. Again, values derived in this fashion will be complicated not only by the complex distribution of the rectangular current to soma and dendrites, but also by the effects of accommodation, synaptic noise and local responses. The latter process will not be apparent when hyperpolarizing pulses are used, and hence the best results may be obtained when this type of pulse is used to block the antidromic invasion of the motoneurone. As is shown in Table 3 by the comparison of column 7 with 5 and 6, the values for four cells derived in this way resemble those derived by strength–latency measurements in being much briefer than those derived from the observed membrane potential changes.

DISCUSSION

The specific membrane resistance (*Table* 4, *column* 5)

It is evident from Table 2, column 2, that, on account of the anatomical configuration of the motoneurone, only a very approximate estimate can be made for the specific membrane resistance. It seems likely that the wide range of the measured resistances for motoneurones (from 0·5 to 2·5 MΩ in Table 1, column 5) is largely attributable to the range of effective surface area, which would be especially related to the number and size of the dendritic branches. As a motoneurone deteriorates, there is a progressive decline both of its membrane potential and its resistance, but the low resistances (under 1·0 MΩ) in Table 1, column 5, cannot be explained in this way, for the membrane potentials of these motoneurones were on the average considerably higher than the remainder, and their spike potentials also indicated that they were in good condition. It seems reasonable to attribute their low resistance to their larger effective area. In so far as a mean value is determinable for the specific membrane resistance of the motoneuronal membrane, it seems that the best approximation is 600 Ω.cm² calculated for a mean resistance of 1·2 MΩ and a standard size of motoneurone with six dendrites (Table 2).

Frank & Fuortes (1956) gave a rather larger value of 1000 Ω.cm² for cat motoneurones, deriving it from their higher mean value for membrane resistance (1·65 MΩ). Still higher values for specific membrane resistance have been determined with other types of nerve cells. Fessard & Tauc (1956) report a mean value of 2200 Ω.cm² for the giant ganglion cells of *Aplysia*, and a value of 500–1000 Ω.cm² is given for the supramedullary neurones of the puffer fish (Hagiwara & Saito, 1957). Since both these measurements were made on cells into which two separate electrodes had been inserted, and which were approximately spherical with no complicating dendrites, they would be the most accurate determinations yet made on nerve cells. Ito's (1957) values on toad spinal ganglion cells also have the merit of being made on spherical cells under direct observation, but only one electrode could be inserted into these much smaller cells, so there was the disability that current had to be passed through the electrode used for making the potential measurements, with the consequent risk of polarization effects. Specific membrane resistances for large and small spinal ganglion cells are shown in Table 4, column 5.

The membrane time constant (*Table* 4, *column* 8)

For the purpose of interpreting the time courses of synaptic action, as attempted in the following paper (Curtis & Eccles, 1959), it is important to have as accurate an estimate as possible of the electric time constant of the motoneuronal membrane. It has been suggested above that Rall (1957) chose too high a value for the specific membrane resistance and hence over-estimated

TABLE 4. Electrical properties of nerve cells

Reference	Cell type	Membrane potential (mV)	R_m Total (MΩ)	R_m Specific (Ω.cm²)	C_m Total (pF)	C_m Specific (μF/cm²)	τ (msec)	Cell area, measurements or assumed (cm²)
1	2	3	4	5	6	7	8	9
Araki & Otani (1955)	Toad motoneurones	−40 to −60	3–6	370	630–1500	—	1·5–8	6×10^{-5}
Frank & Fuortes (1956)	Cat motoneurones	—	1·65 (range 0·7–2·5)	1000	—	1·0–1·5	1·2	5×10^{-4}
This paper	Cat motoneurones	−55 to −80	1·2 (range 0·6–2·5)	600	2500	5	3·1 (range 1·8–5·1)	5×10^{-4}
Rall (1957)	Cat motoneurones	—	—	2000	—	2	4	—
Fessard & Tauc (1957)	*Aplysia* ganglion cells	−40 to −60	2·2	2200	—	23	50 (range 10–80)	—
Ito (1957)	Toad spinal ganglion cells large	−50 to −80	16–22	2200–4000	1900	1·1	2·1–4·6	up to 250×10^{-6}
	Toad spinal ganglion cells small		—	3800–6000	—	2	7·5–12	down to 113×10^{-6}
Hagiwara & Saito (1957)	Supramedullary cells of the puffer fish	−55 to −65	0·6–2·5	500–1000	—	5–15	4–6	—
Otani & Bullock (1957)	Cardiac ganglion cells of lobster	—	0·07–2·6	3000–30,000	—	—	2–16	—

the ratio of dendritic to soma current by a factor of more than 2. As a consequence, from the observed potential changes produced by rectangular currents, he derived an electric time constant of about 4 msec, in contrast to the mean value of 3·1 msec given in Table 3, column 5. In the next paper it will be shown that the lower value allows an interpretation of the time courses of both inhibitory and excitatory post-synaptic potentials that conforms with several other types of experimental investigation, whereas Rall's larger value would lead to considerable difficulties.

As a motoneurone deteriorates, the time constant of the membrane shortens, an effect presumably due to the diminution of the membrane resistance. The values given in Table 3 were recorded from motoneurones as soon as possible after impalement, and results from obviously deteriorated motoneurones were rejected. Nevertheless, it is probable that many of the values listed had already declined considerably below their proper level.

Values for the time constants of different types of nerve cells are shown in Table 4, column 8. It will be seen that spinal ganglion cells are not very different from motoneurones, but the ganglion cells of *Aplysia* have very long time constants. Correspondingly both the excitatory and inhibitory post-synaptic potentials run very prolonged time courses.

The membrane capacity (Table 4, column 7)

The specific membrane capacity is derived by dividing the membrane time constant by the specific membrane resistance; values for several types of neurones are shown in Table 4, column 7. The mean value was about $5\,\mu F/cm^2$ for cat motoneurones. The total effective capacity of a cat motoneurone, as tested by a current applied by an intrasomatic micro-electrode, can likewise be calculated to be about $2{\cdot}5 \times 10^{-9}$ F. A much lower specific membrane capacity ($1{\cdot}0$–$1{\cdot}5\,\mu F/cm^2$) was given by Frank & Fuortes (1956) for cat motoneurones. This discrepancy is largely attributable to the misleading brief value that was derived for the time constant by the strength–latency method (cf. Table 3, column 8).

Specific membrane capacities of $1{\cdot}1$–$2\,\mu F/cm^2$ are reported by Ito (1957) for the toad spinal ganglion cell, which are in approximate agreement with the values of about $1\,\mu F/cm^2$ that obtain for the surface membranes of giant axons. In contrast, much larger values of $23\,\mu F/cm^2$ and 5–$15\,\mu F/cm^2$ have been obtained for the approximately spherical ganglion cells of *Aplysia* and for the supramedullary neurones of the puffer fish.

SUMMARY

1. Rectangular current pulses have been applied to motoneurones through intracellular single or double micro-electrodes and the time courses of the membrane potential changes have been recorded. The most satisfactory

arrangement was to use a double micro-electrode with current passing through one barrel, the potential being recorded through the other. Compensatory circuits are described which balance out artifacts produced by the passage of current through the single or double electrode, at least after the first 1–2 msec. The potential change actually impressed on the motoneuronal membrane is obtained by subtracting the potentials observed when the procedures are repeated with the same balance, but in a just-extracellular position.

2. After the first one or two milliseconds this membrane potential change approaches its final value with a time course that deviates slightly from exponential in that there is a progressive lengthening of successive half-times. The approximate membrane time constant is derived from these curves by allowing for the distribution of applied current between the soma and dendritic membranes (cf. Rall, 1957).

3. The final membrane potential change is approximately proportional to the applied current, the effective membrane resistance being derived from the constant of proportionality. The mean value was 1·2 MΩ (range 0·5–2·5 MΩ).

4. This direct method of measuring membrane resistance is shown usually to give values in approximate agreement with indirect procedures introduced by Frank & Fuortes (1956).

5. The membrane time constant derived from the potential curves (mean value of 3·1 msec, range 1·8–5·1) is much longer than that derived by the strength–latency procedure (mean 1·1 msec). This discrepancy is attributable to several complications that would reduce the latter value below the membrane time constant.

6. Subsidiary methods of measuring membrane time constant are described, which depend on the application of test procedures at various times during a rectangular current pulse.

7. By assuming a standard structure and size for the motoneurones plus dendrites, approximate values have been derived for the specific membrane resistance (600 Ω.cm^2) and capacity (5 μF/cm^2), which are compared with the values obtained by other investigators on motoneurones and other types of nerve cells.

REFERENCES

Adrian, R. H. (1956). The effect of internal and external potassium concentration on the membrane potential of frog muscle. *J. Physiol.* **133**, 631–658.

Araki, T. & Otani, T. (1955). Response of single motoneurones to direct stimulation in toad's spinal cord. *J. Neurophysiol.* **18**, 472–485.

Balthasar, K. (1952). Morphologie der spinalen Tibialis- und Peronaeus-Kerne bei der Katze: Topographie, Architektonik, Axon- und Dendritenverlauf der Motoneurone und Zwischenneurone in den Segmenten L_6–S_2. *Arch. Psychiatr. Z. Neurol.* **188**, 345–378.

Brock, L. G., Coombs, J. S. & Eccles, J. C. (1952). The recording of potentials from motoneurones with an intracellular electrode. *J. Physiol.* **117**, 431–460.

Coombs, J. S., Curtis, D. R. & Eccles, J. C. (1956). Time courses of motoneuronal responses *Nature, Lond.*, **178**, 1049–1050.

COOMBS, J. S., CURTIS, D. R. & ECCLES, J. C. (1957). The generation of impulses in motoneurones. *J. Physiol.* **139**, 232–250.

COOMBS, J. S., ECCLES, J. C. & FATT, F. (1955). The electrical properties of the motoneurone membrane. *J. Physiol.* **130**, 291–325.

DEL CASTILLO, J. & KATZ, B. (1955). Local activity at a depolarized nerve-muscle junction. *J. Physiol.* **128**, 396–411.

CURTIS, D. R. & ECCLES, J. C. (1959). The time courses of excitatory and inhibitory synaptic actions. *J. Physiol.* **145**, 529–547.

ECCLES, J. C., FATT, P., LANDGREN, S. & WINSBURY, G. J. (1954). Spinal cord potentials generated by volleys in the large muscle afferents. *J. Physiol.* **125**, 590–606.

ECCLES, J. C., LIBET, B. & YOUNG, R. R. (1958). The behaviour of chromatolysed motoneurones studied by intracellular recording. *J. Physiol.* **143**, 11–40.

FATT, P. & KATZ, B. (1951). Analysis of the end-plate potential recorded with an intra-cellular electrode. *J. Physiol.* **115**, 320–370.

FESSARD, A. & TAUC, L. (1956). Capacité, résistance et variations actives d'impédance d'un soma neuronique. *J. Physiol. Path. gén.* **48**, 541–544.

FRANK, K. & FUORTES, M. G. F. (1956). Stimulation of spinal motoneurones with intracellular electrodes. *J. Physiol.* **134**, 451–470.

HAGIWARA, S. & SAITO, N. (1957). Mechanism of action potential production in the nerve cell of a Puffer. *Proc. Japan. Academy*, **33**, 682–685.

HODGKIN, A. L. (1951). The ionic basis of electrical activity in nerve and muscle. *Biol. Rev.* **26**, 339–409.

HODGKIN, A. L. & HUXLEY, A. F. (1952). A quantitative description of membrane current and its application to conduction and excitation in nerve. *J. Physiol.* **117**, 500–544.

HODGKIN, A. L. & RUSHTON, W. A. H. (1946). The electrical constants of a crustacean nerve fibre. *Proc. Roy. Soc.* B, **133**, 444–479.

ITO, M. (1957). The electrical activity of spinal ganglion cells investigated with intracellular microelectrodes. *Jap. J. Physiol.* **7**, 297–323.

JENERICK, H. P. & GERARD, R. W. (1953). Membrane potential and threshold of single muscle fibres. *J. cell. comp. Physiol.* **42**, 79–102.

KATZ, B. (1948). The electrical properties of the muscle fibre membrane. *Proc. Roy. Soc.* B, **135**, 506–534.

OTANI, T. & BULLOCK, T. H. (1957). Responses to depolarizing currents across the membrane of some invertebrate ganglion cells. *Anat. Rec.*, **128**, 599.

RALL, W. (1955). A statistical theory of monosynaptic input-output relations. *J. cell. comp. Physiol.* **46**, 373–411.

RALL, W. (1957). Membrane time constant of motoneurones. *Science*, **126**, 454.

TAUC, L. (1955). Étude de l'activité élémentaire des cellules du ganglion abdominal de l'Aplysie. *J. Physiol. Path. gén.* **47**, 769–792.

TAUC, L. (1956). Potentiels sous-liminaires dans le soma neuronique de l'Aplysie et de l'Escargot. *J. Physiol. Path. gén.* **48**, 715–718.

TAUC, L. (1957). Les divers modes d'activité du soma neuronique gangliönnaire de l'Aplysie et de l'Escargot. *Colloques Internationaux du centre National de la Recherche Scientifique.* No. 67, pp. 91–119.

WEIDMANN, S. (1955). The effect of the cardiac membrane potential on the rapid availability of the sodium-carrying system. *J. Physiol.* **127**, 213–224.